Article

Cell Reports

# Multifaceted Impact of MicroRNA 493-5p on Genome-Stabilizing Pathways Induces Platinum and PARP Inhibitor Resistance in *BRCA2*-Mutated Carcinomas

## Graphical Abstract

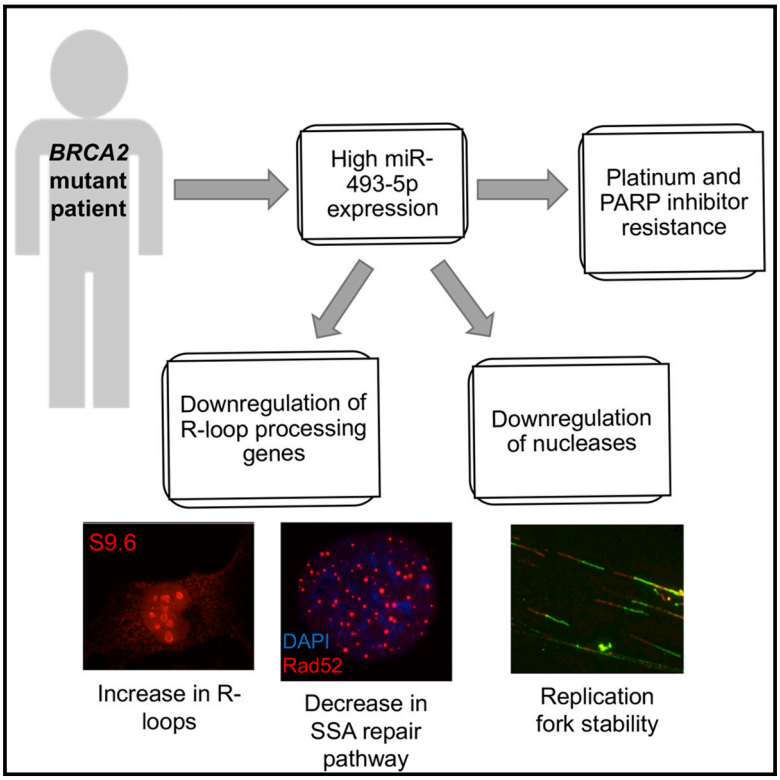


## Authors

Khyati Meghani, Walker Fuchs, Alexandre Detappe, ..., Elizabeth M. Swisher, Panagiotis A. Konstantinopoulos, Dipanjan Chowdhury

## Correspondence

panagiotis_konstantinopoulos@dfci.harvard.edu (P.A.K.), dipanjan_chowdhury@dfci.harvard.edu (D.C.)

## In Brief

Meghani et al. find that increased expression of miR-493-5p induces resistance to platinum and PARP inhibitors in patient cells harboring *BRCA2* mutations by targeting repair pathways involved in maintaining genome stability.

## Highlights

- miR-493-5p induces resistance to PARPi and platinum in *BRCA2* mutant cells
- miR-439-5p expression correlates with disease-free survival in *BRCA2* mutant patients
- miR-493-5p overexpression protects replication fork from nuclease degradation
- High miR-493-5p expression decreases repair by the mutagenic SSA repair pathway

Meghani et al., 2018, Cell Reports *23*, 100–111
April 3, 2018 
https://doi.org/10.1016/j.celrep.2018.03.038

CellPress

OPEN ACCESS
CellPress

Cell Reports
Article

# Multifaceted Impact of MicroRNA 493-5p on Genome-Stabilizing Pathways Induces Platinum and PARP Inhibitor Resistance in *BRCA2*-Mutated Carcinomas

Khyati Meghani,[1] Walker Fuchs,[1,6] Alexandre Detappe,[2,6] Pascal Drané,[1] Ewa Gogola,[3] Sven Rottenberg,[3,4] Jos Jonkers,[3] Ursula Matulonis,[2] Elizabeth M. Swisher,[5] Panagiotis A. Konstantinopoulos,[2,*] and Dipanjan Chowdhury[1,7,*]

[1]Department of Radiation Oncology, Division of Radiation and Genome Stability, Dana-Farber Cancer Institute, Harvard Medical School, Boston, MA, USA

[2]Department of Medical Oncology, Dana-Farber Cancer Institute, Harvard Medical School, Boston, MA, USA

[3]Division of Molecular Pathology and Cancer Genomics Netherlands, The Netherlands Cancer Institute, Plesmanlaan 121, 1066 CX Amsterdam, the Netherlands

[4]Institute of Animal Pathology, Vetsuisse Faculty, University of Bern, Laenggassstr. 122, 3012 Bern, Switzerland

[5]Division of Gynecologic Oncology, Department of Obstetrics and Gynecology, University of Washington, Seattle, WA, USA

[6]These authors contributed equally

[7]Lead Contact

*Correspondence: panagiotis_konstantinopoulos@dfci.harvard.edu (P.A.K.), dipanjan_chowdhury@dfci.harvard.edu (D.C.)

https://doi.org/10.1016/j.celrep.2018.03.038

## SUMMARY

***BRCA1/2*-mutated ovarian cancers (OCs) are defective in homologous recombination repair (HRR) of double-strand breaks (DSBs) and thereby sensitive to platinum and PARP inhibitors (PARPis). Multiple PARPis have recently received US Food and Drug Administration (FDA) approval for treatment of OCs, and resistance to PARPis is a major clinical problem. Utilizing primary and recurrent *BRCA1/2*-mutated carcinomas from OC patients, patient-derived lines, and an *in vivo BRCA2*-mutated mouse model, we identified a microRNA, miR-493-5p, that induced platinum/PARPi resistance exclusively in *BRCA2*-mutated carcinomas. However, in contrast to the most prevalent resistance mechanisms in *BRCA* mutant carcinomas, miR-493-5p did not restore HRR. Expression of miR-493-5p in *BRCA2*-mutated/depleted cells reduced levels of nucleases and other factors involved in maintaining genomic stability. This resulted in relatively stable replication forks, diminished single-strand annealing of DSBs, and increased R-loop formation. We conclude that impact of miR-493-5p on multiple pathways pertinent to genome stability cumulatively causes PARPi/platinum resistance in *BRCA2* mutant carcinomas.**

## INTRODUCTION

Large-scale genomic studies have demonstrated that approximately 50% of high-grade serous ovarian carcinomas (HGSOCs) harbor genetic and/or epigenetic alterations in homologous recombination repair (HRR) pathway genes (Cancer Genome Atlas Research Network, 2011), most commonly in *BRCA1* and *BRCA2* (Konstantinopoulos et al., 2015; Lord and Ashworth, 2016). Loss of HRR causes genomic instability, hyper-dependence on alternative DNA repair mechanisms, and enhanced sensitivity to certain types of DNA-damaging chemotherapy, such as platinum analogs and topoisomerase inhibitors (Evers et al., 2010; Konstantinopoulos et al., 2015). HRR-deficient cancers are also exquisitely sensitive to PARP inhibitors (PARPis), which exhibit synthetic lethality to cells with defective HRR. This synthetic lethal interaction is being exploited therapeutically in ovarian carcinoma whereby three PARPis, i.e., olaparib, rucaparib, and niraparib, have received US Food and Drug Administration (FDA) approval as monotherapy in patients with germline or somatic *BRCA1/2* mutations or as maintenance therapy after platinum chemotherapy in platinum-sensitive recurrent ovarian carcinoma (Konstantinopoulos et al., 2015; Matulonis et al., 2016; Mirza et al., 2016; Swisher et al., 2017). The efficacy of PARPis against HRR-deficient cells can be explained by several mechanisms, including inhibition of base excision repair (BER), trapping of PARP-DNA complexes at the replication fork, enhancement of toxic classic non-homologous end joining (NHEJ), and inhibition of PARP1/Polθ-mediated alternative end joining (alt-EJ) (Konstantinopoulos et al., 2015).

Despite their predicted synthetic lethality, a large fraction of carcinomas eventually become resistant to these therapies. Underlying HRR deficiency is important for the cytotoxicity of PARPis and platinum agents, and this is highlighted by the fact that the most prevalent mechanisms of resistance to these therapies are secondary somatic *BRCA1/2* mutations that restore the open reading frame and re-establish HRR proficiency (Sakai et al., 2008; Swisher et al., 2008). Besides reversion mutations, there are few clinically relevant mechanisms that have been identified. In *BRCA1*-mutated carcinomas, PARPi and platinum resistance may also occur via suppression of NHEJ, which also restores HRR proficiency. Loss of NHEJ confers resistance only to *BRCA1* mutant carcinomas as *BRCA1* is required in the early steps of HRR, and it may be "bypassed" either by loss of

*53BP1* or loss of *REV7* or via downregulation of the *Ku70/Ku80* complex, which has been shown to restore competent HRR in *BRCA1*-deficient cells (Aly and Ganesan, 2011; Bouwman et al., 2010; Bunting et al., 2010; Xu et al., 2015). Identifying the mechanism of platinum and PARPi resistance in *BRCA2*-mutated carcinomas has been a challenge as HRR is not restored in cells expressing mutant *BRCA2*. However, few recent studies have revealed that *BRCA2* mutant carcinomas might still develop platinum and PARPi resistance without restoration of HRR proficiency via a complex mechanism where stalled DNA replication fork is protected from degradation by nucleases by downregulation of proteins such as *PTIP*, *CHD4*, or *EZH2* (Guillemette et al., 2015; Lai et al., 2017; Patch et al., 2015; Ray Chaudhuri et al., 2016; Rondinelli et al., 2017). Importantly, it is not clear how these factors would be downregulated in *BRCA2* mutant cancers.

We have been systematically studying the role of microRNAs (miRNAs) in HRR and their role in mediating PARPi sensitivity (Choi et al., 2014, 2016; Moskwa et al., 2011). In this regard, using a candidate-based approach, we have recently shown that overexpression of a miRNA, miR-622, induces resistance to PARPi and platinum-based drugs in *BRCA1* mutant ovarian carcinomas (Choi et al., 2016). We observed that miR-622 regulated the expression of the Ku complex and suppressed NHEJ, thereby rescuing the HRR deficiency of *BRCA1* mutant ovarian carcinomas and induced resistance to PARPi and platinum-based drugs.

To systematically identify clinically relevant miRNAs that mediate platinum and PARPi resistance in *BRCA1/2*-mutated cancers, we performed next-generation sequencing of small RNAs extracted from the tumors of 38 patients with primary and recurrent *BRCA1/2*-mutated ovarian carcinomas. The results of the small RNA sequencing were independently validated in The Cancer Genome Atlas (TCGA) dataset and revealed a miRNA, miR-493-5p, as a mediator of resistance to platinum and PARPis exclusively in *BRCA2*-mutated ovarian carcinomas. We have characterized the functional impact of miR-493-5p in *BRCA2*-mutated cancer cells and demonstrated that it induces platinum and PARPi resistance by influencing multiple genome-stabilizing pathways that include single-strand annealing (SSA), R-loops, and replication fork stability.

## RESULTS

### Small RNA Sequencing of *BRCA1/2*-Mutated Ovarian Carcinomas Identifies Several miRNAs as Possible Mediators of Platinum Resistance

We performed next-generation sequencing of small RNAs extracted from the tumors of 38 patients with primary and recurrent *BRCA1/2*-mutated ovarian carcinomas. None of these carcinomas harbored *BRCA1/2* reversion mutations, as we wanted to focus on mechanisms of resistance that were unrelated to secondary *BRCA1/2* mutations. Our analysis focused on miRNAs that fulfilled two criteria: (1) were differentially expressed between platinum-resistant/refractory and platinum-sensitive *BRCA1/2*-mutated carcinomas and (2) their expression was concordantly associated with outcome after platinum therapy among *BRCA1/2*-mutated carcinomas.

Eight miRNAs, miR-139-5p, miR-493-5p, miR-378a-5p and miR-491-5p, miR-5000-3p, miR-369-3p, miR-3188, and miR-141-3p were identified to fulfill these criteria. Five of these miRNAs, miR-139-5p, miR-493-5p, miR-3188, miR-369-3p, and miR-5000-3p were overexpressed ($p < 0.05$) in platinum-resistant/refractory *BRCA1/2*-mutated carcinomas compared to platinum-sensitive *BRCA1/2*-mutated carcinomas and were associated with worse outcome after platinum therapy (Figures 1A and S1A). Conversely, the other three miRNAs, miR-141-3p, miR-378a-5p, and miR-491-5p, were under-expressed ($p < 0.05$) in platinum-resistant/refractory *BRCA1/2*-mutated carcinomas compared to platinum-sensitive *BRCA1/2*-mutated carcinomas and were associated with better outcome after platinum therapy (Figures 1A and S1A).

We then explored whether the impact of each of these 8 miRNAs was specific for *BRCA1*- or *BRCA2*-mutated carcinomas. Strikingly, the effect of miR-493-5p (Figure 1B) and miR-491-5p (Figure S1B) on outcome was only evident in *BRCA2*-mutated carcinomas, whereas the effect of miR-378a-5p, miR-3188, and miR-141-3p was evident only in *BRCA1*-mutated carcinomas (Figure S1B). Effect of miR-5000-3p, miR-139-5p, and miR-369-3p was not specific for *BRCA1*- or *BRCA2*-mutated carcinomas (Figure S1B).

### Independent Validation of Small RNA Sequencing Findings for miR-493-5p in TCGA Dataset

TCGA dataset was queried to independently validate the findings of the small RNA sequencing. All patients included in TCGA cohort were diagnosed with HGSOC and underwent surgery followed by platinum-based chemotherapy. miR-139-5p, miR-493-5p, miR-378a-5p and miR-491-5p, miR-369-3p, and miR-141-3p were queried for their impact on survival in *BRCA1*- and *BRCA2*-mutated HGSOC using quartile cutoff to segregate carcinomas with high, intermediary, and low miRNA expression. (TCGA miRNA expression data were not available for miR-3188 and miR-5000-3p). HGSOC with miRNA expression levels below 25% were classified as low expression, HGSOC with levels between 25% and 75% quartile were classified as intermediary expression, and HGSOC with miRNA levels above 75% quartile were classified as high expression.

Of the 6 miRNAs identified in the small RNA sequencing, only miR-493-5p was associated with outcome in TCGA dataset. Specifically, in resonance with the observations from the RNA sequencing, overexpression of miR-493-5p (Figure 1C) was associated with worse outcome after platinum chemotherapy in *BRCA2*-mutated carcinomas of TCGA dataset, but not in *BRCA1*-mutated carcinomas. We did not observe an association between miR-139-5p, miR-378a-5p and miR-491-5p, miR-369-3p, and miR-141-3p levels and survival outcome in either the *BRCA1*-mutated or the *BRCA2*-mutated HGSOCs of TCGA dataset (Figure S1C).

To evaluate the impact of miR-493-5p on tumor regression, we queried miR-493-5p expression levels in carcinomas classified into 2 groups based on the amount of residual tumors detected post-debulking surgery (group A: cases with no residual tumors detected, 1–10 mm residual tumors; group B: cases with 11–20 mm and >20 mm residual tumors detected). We did not observe a significant difference in miR-493-5p expression levels

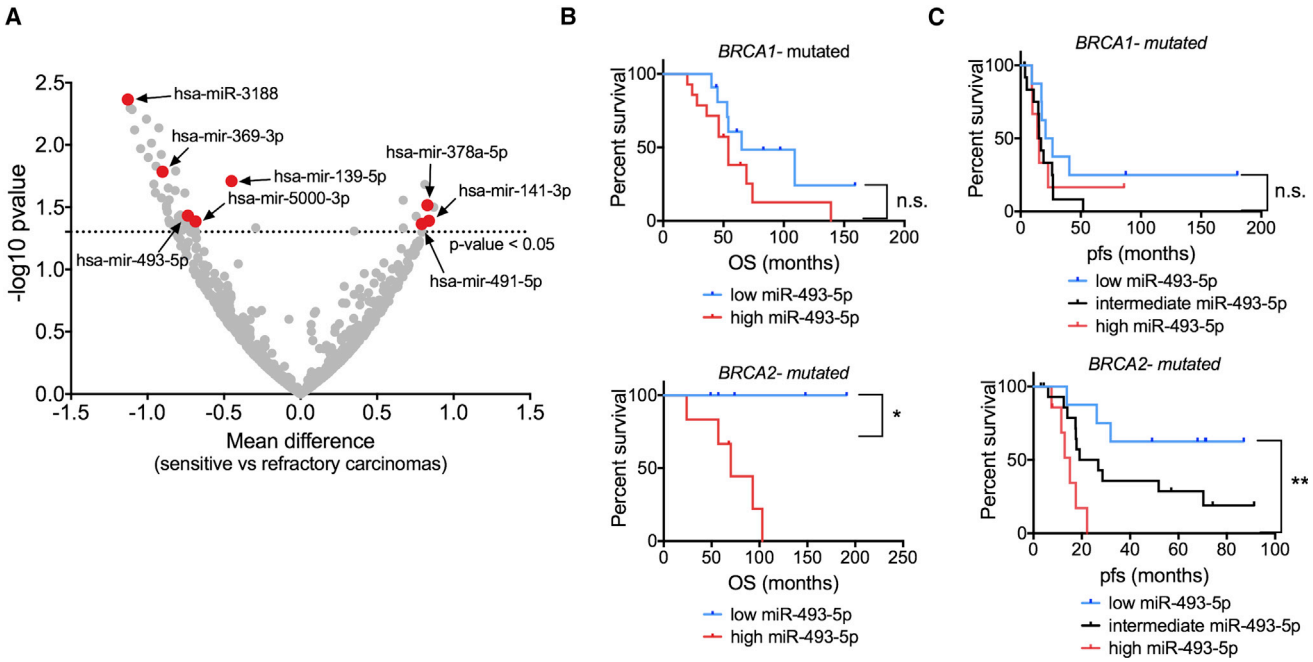


**Figure 1. Expression of miR-493-5p Correlates with Platinum-Resistant/Refractory Disease Specifically in *BRCA2* Mutant Ovarian Carcinomas**

(A) Volcano plot representing differentially expressed miRNAs in platinum-sensitive versus platinum-resistant/refractory carcinomas. x axis represents mean difference in miRNA expression (sensitive versus resistant), and y axis represents ANOVA p value (−log10).

(B) Overall survival (OS) for patients with *BRCA1*- or *BRCA2*-mutated ovarian carcinomas based on above or below median expression values of miR-493-5p. Left panel denotes overall survival for *BRCA1*-mutated tumors. Right panel denotes overall survival for *BRCA2*-mutated tumors. Statistical significance was assessed by the log rank test.

(C) Progression-free survival (PFS) for patients with *BRCA1*- or *BRCA2*-mutated HGSOCs based on quartile cutoff expression values of miR-493-5p. Left panel denotes progression-free survival for *BRCA1*-mutated carcinomas. Right panel denotes progression-free survival for *BRCA2*-mutated carcinomas. Statistical significance was assessed by the log rank test.

For all panels, n.s. represents p value > 0.05, *p value < 0.05, **p value < 0.01, ***p value < 0.001, and ****p value < 0.0001. See also Figure S1.

between the two groups. Furthermore, multivariate survival analysis with miR-493-5p expression levels and amount of tumor detected post-surgery as covariates in BRCA2-mutated carcinomas showed significant impact of miR-493-5p expression on survival but no association between disease-free survival and the amount of residual tumor detected. In *BRCA1*-mutated tumors, no significant association was observed with miR-493-5p expression levels and amount of residual tumor (Figure S1D). Taken together, the results from the small RNA sequencing and TCGA dataset suggest that miR-493-5p may be a mediator of platinum resistance in *BRCA2*-mutated ovarian carcinomas.

## miR-493-5p Mediates Resistance to Platinum and PARPi in *BRCA2* Mutant, but Not *BRCA1* Mutant, Models *In Vitro*

We evaluated the impact of miR-493-5p on PARPi and platinum sensitivity in a panel of patient-derived *BRCA1*-mutated (COV362 and UWB1.289) and *BRCA2*-mutated ovarian cancer cell lines (OVSAHO and Kuramochi) and in *BRCA2* mutant VU423 fibroblast cells. As shown in Figure 2A, overexpression of miR-493-5p is associated with cisplatin and olaparib resistance, causing significant increase in the half maximal inhibitory concentration ($IC_{50}$) for cisplatin and olaparib in *BRCA2* mutant OVSAHO, Kuramochi, and VU423 cells. miR-493-5p overexpression is also associated with resistance to PARPi rucaparib and alkylating agent carboplatin in *BRCA2* mutant VU423 cells (Figure S2A). Conversely, in agreement with the small RNA sequencing data and TCGA findings, overexpression of miR-493-5p had no effect on cisplatin and olaparib sensitivity in *BRCA1*-mutated COV362 and UWB1.289 cells (Figure 2B). Additionally, antagonizing endogenous miR-493-5p significantly sensitized *BRCA2* mutant OVSAHO, Kuramochi, and VU423 cells to cisplatin and olaparib (Figure S2B).

## miR-493-5p Is Upregulated in a *Brca2*-Mutated Mammary Tumor Model with Acquired PARPi Resistance *In Vivo*

To determine whether overexpression of miR-493-5p could be a possible mechanism of acquired resistance in *BRCA2*-mutated cancers, we utilized the unique genetically engineered mouse (GEM) KB2P mouse model for *Brca2*-deficient breast cancer (Jaspers et al., 2015; Jonkers et al., 2001). This model harbors large intragenic deletion in *Brca2*; therefore, acquired resistance to PARPis in this model cannot occur via secondary *Brca2* mutations. Tumors from KB2P mouse donors were transplanted orthotopically into wild-type syngeneic mice, and when the tumor

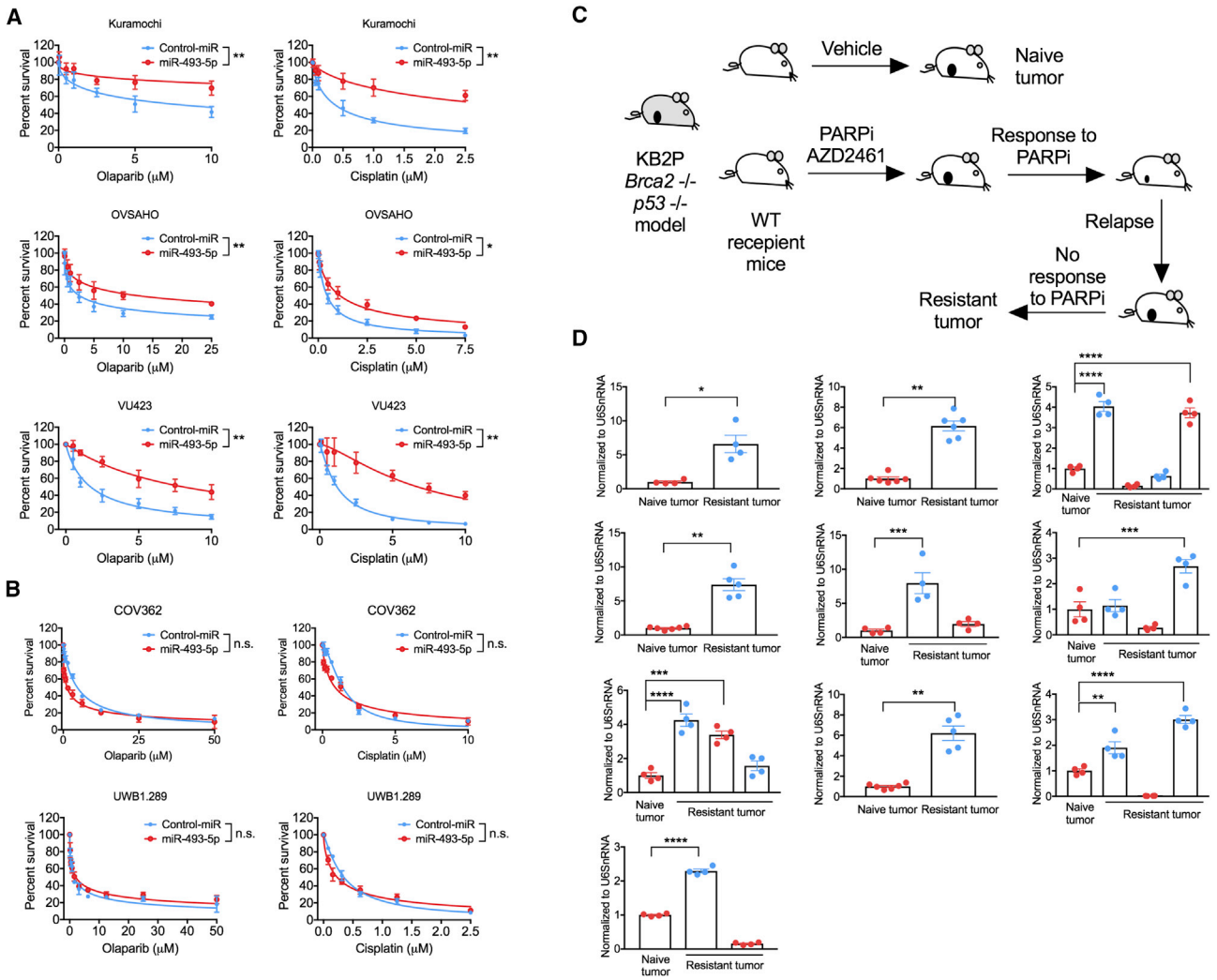


**Figure 2. Expression of miR-493-5p Causes PARPi and Platinum Resistance in *BRCA2* Mutant Cells *In Vitro* and *In Vivo***

(A) Survival assays to examine the impact of miR-493-5p overexpression in *BRCA2* mutant KURAMOCHI, OVSAHO, and VU423 cells exposed to the indicated DNA-damaging agents.

(B) Survival assays to examine the impact of miR-493-5p overexpression in *BRCA1* mutant COV362 and UWB1.289 cells exposed to the indicated DNA-damaging agents.

(C) Schematic for KB2P (*p53*−/− *Brca2*−/− mouse model) PARPi intervention study.

(D) miR-493-5p expression levels in matched PARPi-naive and resistant KB2P p53−/− *Brca2*−/− mammary mouse models (derived from independent spontaneous tumor donors). Expression was normalized using U6SnRNA as reference.

For all panels, data are represented as mean ± SEM from three different experiments, n.s. represents p value > 0.05, *p value < 0.05, **p value < 0.01, ***p value < 0.001, and ****p value < 0.0001. See also Figure S2.

reached a volume >200 $mm^3$, mice were treated with the PARPi AZD2461 for 28 consecutive days. Of note, PARPi AZD2461 is not a P-glycoprotein (Pgp) substrate, and therefore, acquired resistance to AZD2461 cannot be mediated by Pgp upregulation (Oplustil O'Connor et al., 2016). After an initial phase of response, the tumors eventually relapsed and were allowed to regrow to 100% volume, following which another treatment cycle was started. Eventually, upon repeated exposure, mouse models with acquired resistance to PARPi AZD2461 were generated. Each untreated naive tumor had either one or more matched resistant counterparts (Figure 2C). Out of 40 resistant tumor models generated from 19 untreated naive tumors, we observed a statistically significant increase in miR-493-5p levels in 13 of them (32.5%; 90% confidence interval [CI]: 20.4%–40.6%; Figure 2D).

## Microarray Profiling to Identify Gene Targets of miR-493-5p

Given the potential of miRNAs to regulate multiple mRNA transcripts, we utilized an unbiased approach to identify gene targets for miR-493-5p. Accordingly, we used the HTA2.0 (Affymetrix) microarray platform to profile whole transcriptome

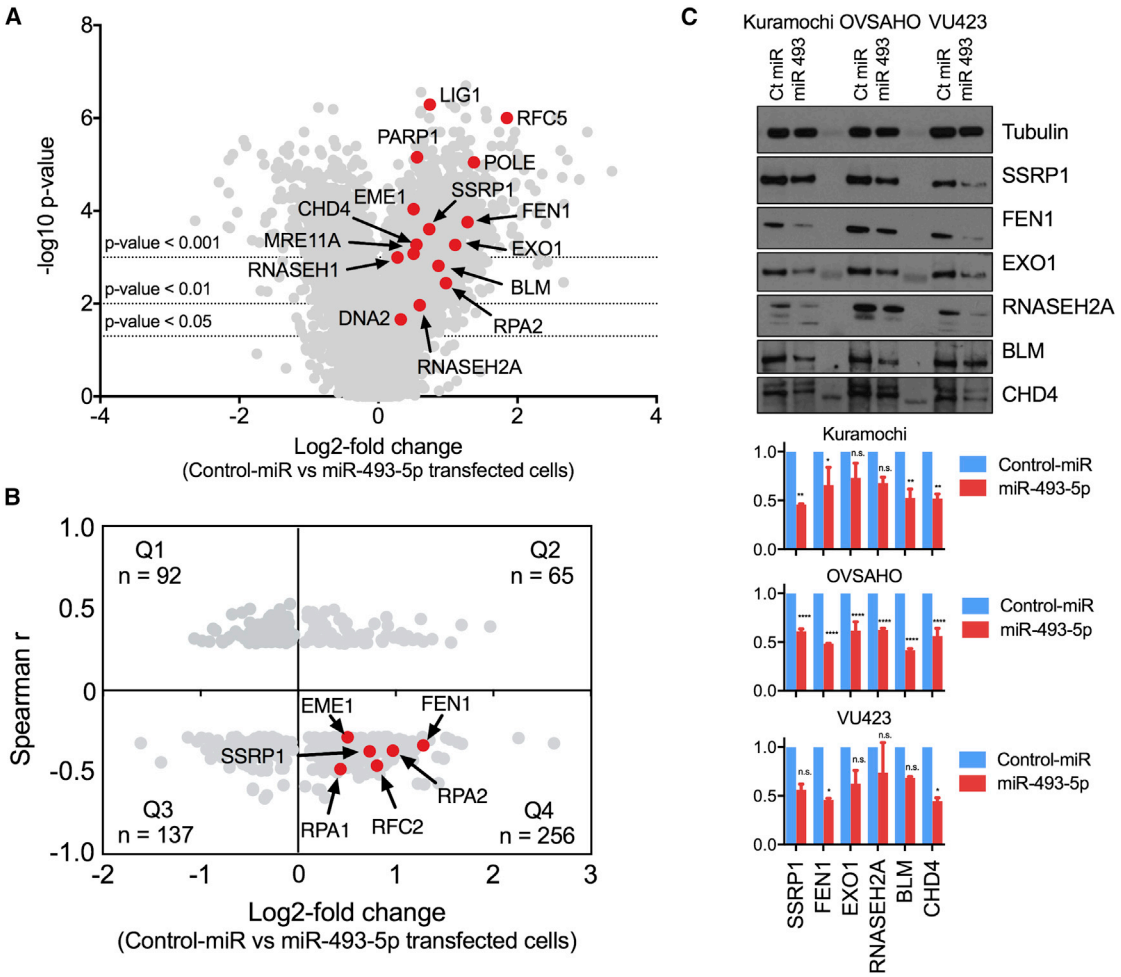


**Figure 3. miR-493-5p Significantly Downregulates Expression of Multiple Genes Involved in Genomic Stability**

(A) Volcano plot depicting differentially expressed genes in control-miR versus miR-493-5p-overexpressing Kuramochi cells. x axis represents log2 expression fold change in control-miR versus miR-493-5p-mimic-transfected cells, and the y axis represents ANOVA p value (−log10).

(B) Quadrant-based segregation to identify genes that are significantly differentially expressed in the microarray and significantly correlate to levels of miR-493-5p in *BRCA2*-mutated carcinomas in the TCGA dataset. Highlighted quadrant four represents 245 genes that are significantly downregulated in the microarray and correlate significantly to miR-493-5p levels in the TCGA cohort of 34 *BRCA2*-mutated tumors.

(C) Quantification of protein levels in miR-493-5p-transfected cells normalized to control-miR-transfected cells.

For (C), data are represented as mean ± SEM from two different experiments, n.s. represents p value > 0.05, *p value < 0.05, **p value < 0.01, ***p value < 0.001, and ****p value < 0.0001. See also Figure S3.

changes in *BRCA2*-mutated Kuramochi cells, transfected with either control-miRNA or miR-493-5p mimics (Figure 3A). Comparison was performed between gene expression levels in control versus miR-493-5p transfected cells, with a statistical significance criterion of p value < 0.05 and a false discovery rate cutoff of <0.2. We performed gene set enrichment analysis (GSEA) on the significant hits and identified several pathways that play a key role in DNA replication and repair among the top hits to be downregulated in miR-493-5p-overexpressing cells (Table S1). To better define miR-493-5p-responsive pathways, we performed miRNA-mRNA correlation analysis for *BRCA2*-mutated tumors in TCGA dataset and identified 256 genes (Figure 3B) that were both (1) significantly overexpressed in control-miRNA transfected compared to miR-493-5p mimic transfected Kuramochi cells and (2) inversely correlated with miR-493-5p levels among the *BRCA2*-mutated carcinomas in the TCGA dataset. A few genes that fit these criteria (*FEN1*, *SSRP1*, and *EME1*) have been implicated in maintenance of genome stability. However, there were also several genes (*MRE11*, *BLM*, *EXO1*, and *CHD4*) that had a very striking difference in our transcriptomic analysis but did not meet the statistical significance cutoff for inverse correlation with miR-493-5p in TCGA (Figure S3). To delineate the mechanism behind the observed decrease in transcript levels, we queried publicly available databases and identified miRNA binding sites for these genes (Table 1). Subsequently, we assessed the impact of miR-493-5p on the protein levels of all these genes (*SSRP1*, *FEN1*, *EXO1*, *RNASEH2A*, *BLM*, and

**Table 1. miR-493-5p Binding Sites in the Genomic Sequences of the Indicated Genes Predicted Using the RNA 22 Version 2.0 Algorithm**

| | | | | | | | | | | | | | | | | | | | | | | |
|---|---|---|---|---|---|---|---|---|---|---|---|---|---|---|---|---|---|---|---|---|---|---|
| U | U | A | C | U | U | U | C | G | G | A | U | G | G | U | A | C | A | U | G | U | U | hsa-mir-493-5p |
| | | | | | \| | \| | \| | \| | \| | | \| | \| | \| | | \| | \| | \| | : | \| | \| | | | |
| U | C | C | A | C | A | A | G | C | C | - | A | C | C | - | U | G | U | G | C | A | C | SSRP1 |
| U | U | A | C | U | U | U | C | G | G | A | U | G | G | U | A | C | A | U | G | U | U | hsa-miR-493-5p |
| | | | \| | : | \| | : | | \| | | | \| | | | \| | \| | \| | \| | \| | | | |
| G | G | G | G | G | A | G | A | C | A | A | A | A | G | A | U | G | U | A | C | A | G | FEN1 |
| U | U | A | C | U | U | U | C | G | G | A | U | G | G | U | A | C | A | U | G | U | U | hsa-miR-493-5p |
| | | | | | | | \| | \| | | | : | \| | \| | \| | \| | | \| | : | \| | \| | : |
| A | G | C | G | C | U | G | G | C | - | - | G | C | C | A | U | C | U | G | C | A | G | CHD4 |
| U | U | A | C | U | U | U | C | G | G | A | U | G | G | U | A | C | A | U | G | U | U | hsa-miR-493-5p |
| | | | | | | \| | \| | \| | : | | | \| | \| | | \| | \| | \| | \| | \| | : |
| C | C | C | C | A | C | A | G | C | U | - | - | C | C | U | G | G | U | A | C | A | G | EME1 |
| U | U | A | C | U | U | U | C | G | G | A | U | G | G | U | A | C | A | U | G | U | U | hsa-miR-493-5p |
| | | | \| | \| | : | \| | | \| | \| | | | | \| | \| | | \| | \| | \| | | : | | | |
| A | A | G | G | A | G | A | A | C | C | - | - | A | C | A | C | G | U | A | G | G | G | RNASEH2A |
| U | U | A | C | U | U | U | C | G | G | A | U | G | G | U | A | C | A | U | G | U | U | hsa-miR-493-5p |
| \| | : | \| | \| | | | | | | \| | \| | : | \| | | | \| | \| | \| | \| | \| | \| | \| | |
| A | G | U | G | U | U | A | C | U | G | C | A | U | U | U | U | G | U | A | C | A | A | RPA2 |
| U | U | A | C | U | U | U | C | G | G | - | - | A | U | G | G | U | A | C | A | U | G | U | U | hsa-miR-493-5p |
| | | | | | | | \| | \| | : | | | \| | : | \| | \| | \| | \| | \| | \| | \| | \| | \| |
| A | U | A | A | C | U | U | G | C | U | G | U | U | G | C | C | A | U | G | U | A | C | A | U | MRE11A |
| U | U | A | C | U | U | U | C | G | G | A | U | G | - | - | G | U | A | C | A | U | G | U | U | hsa-miR-493-5p |
| | | | | \| | | \| | \| | | | \| | \| | \| | | | | | | \| | \| | \| | \| | : | \| | |
| A | A | A | A | A | U | A | G | A | A | U | A | C | A | U | U | U | U | G | U | A | U | A | U | EXO1 |
| U | U | A | C | U | U | U | C | - | G | G | A | U | G | - | G | U | A | C | A | U | G | U | U | hsa-miR-493-5p |
| | | | | : | \| | \| | \| | | | | \| | \| | \| | | \| | \| | \| | \| | | | \| | \| | |
| A | G | A | A | G | A | A | G | A | A | A | U | A | C | A | C | A | U | G | C | U | C | A | U | BLM |

*CHD4*) in three *BRCA2* mutant cell lines. Consistent with our mRNA analysis, we observed a decrease in protein levels of these factors in multiple *BRCA2* mutant cell lines transfected with the miR-493-5p mimic (Figure 3C). Having established the impact of miR-493-5p on these transcripts, next we decided to investigate the relevance of our identified targets by querying the impact of miR-493-5p on different repair pathways where these factors are known to play an important role.

### miR-493-5p Decreases SSA in *BRCA2*-Mutated Cells and Does Not Rescue HRR

The primary mechanism by which *BRCA* mutant ovarian carcinomas develop platinum or PARPi resistance is by the restoration of HRR (Norquist et al., 2011; Sakai et al., 2008, 2009). Additionally, a recent study (Feng and Jasin, 2017) has used separation-of-function BRCA2 mutants to demonstrate that the impact of *BRCA2* on cell viability is primarily mediated by it function in HRR and not replication fork stability. Therefore, we explored the impact of miR-493-5p on HRR using the HDR reporter substrate (DR-GFP) reporter assay. *BRCA2* knockdown in the DR-GFP system showed a decrease in HRR efficiency as expected; however, we did not observe a rescue in HRR upon overexpression of miR-493-5p after *BRCA2* knockdown (Figure 4A). As an additional readout for HRR, we performed Rad51 foci formation assay in *BRCA1/2*-wild-type U2OS cells (Figure 4B) and in *BRCA2* mutant VU423 and Kuramochi cells (Figures S4A and S4B). As with the results obtained with the DR-GFP system, overexpression of miR-493-5p caused a moderate decrease in Rad51 foci in wild-type U2OS cells but did not rescue HRR in *BRCA2*-mutated VU423 and Kuramochi cells. The SSA repair pathway is distinct as it distinguishes *BRCA1* and *BRCA2* mutant cells. *BRCA1* mutant cells exhibit diminished HRR and SSA, whereas *BRCA2* mutant cells have impaired HHR but a hyperactive SSA repair pathway, which is responsible for increased chromosomal aberrations in these cells (Stark et al., 2004). To study SSA, we utilized a previously reported SSA reporter pathway system (Bennardo et al., 2008; Stark et al., 2004). In agreement with published reports, we observed a significant escalation in SSA upon *BRCA2* loss (Figure 4A). However, in cells with silenced *BRCA2*, overexpression of miR-493-5p was associated with a significant decrease in SSA (Figure 4A). As an additional readout for SSA, we created a stable VU423 cell line expressing mCherry-tagged Rad52. In concordance with the results in reporter cells, we also observed a significant decrease in Rad52 foci upon overexpression of miR-493-5p (Figure 4C). We also assessed whether miR-493-5p

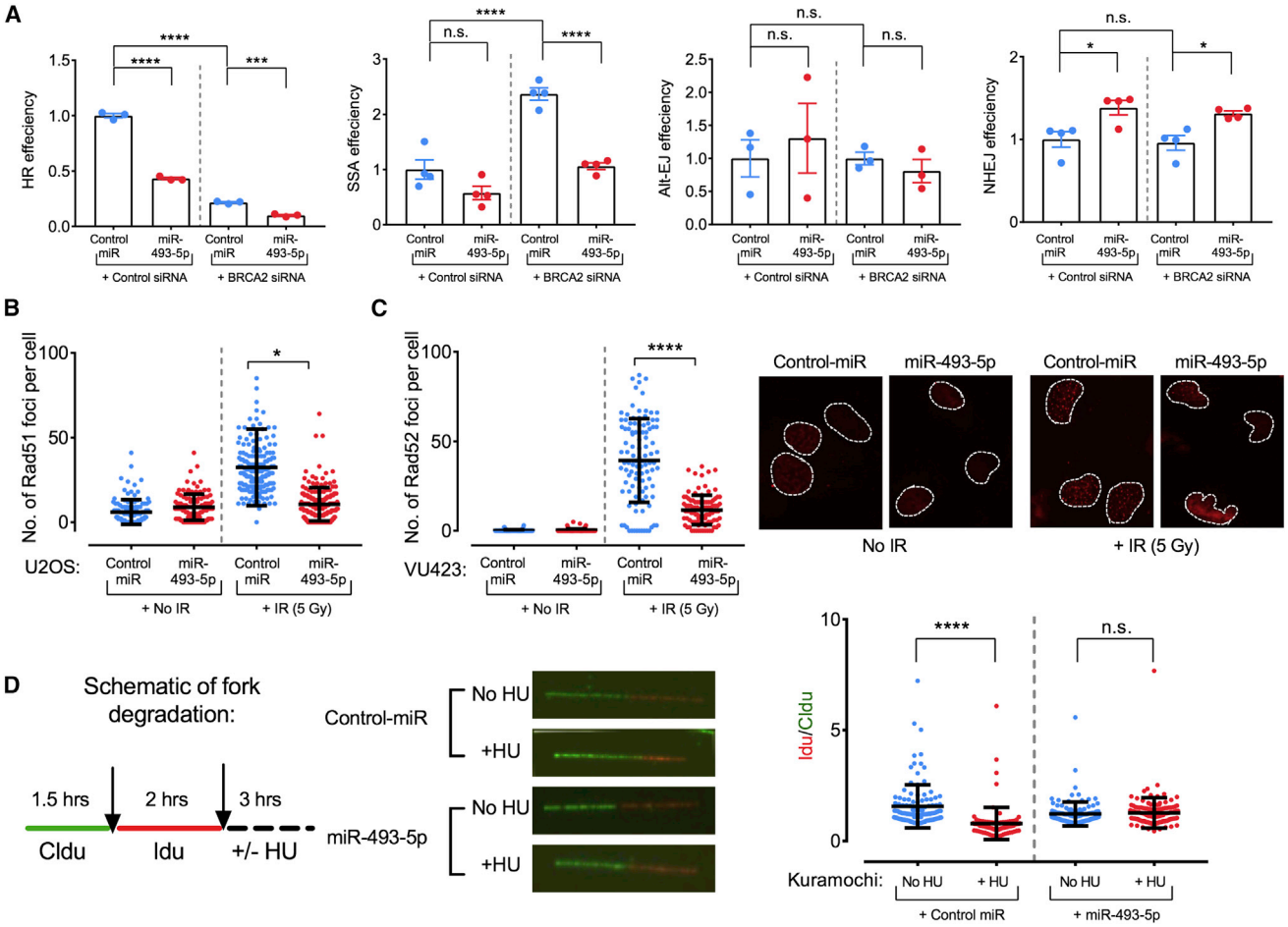


**Figure 4. miR-493-5p Has an Impact on SSA, DNA Replication Fork Stability in *BRCA2* Mutant, or Depleted Cells**

(A) DR-GFP, SA-GFP, EJ-2, and EJ-5 assay in U2OS cells transfected with indicated siRNA or miRNA.

(B) Quantification of Rad51 foci dynamics in U2OS cells transfected with the indicated miRNA.

(C) Quantification of Rad52 foci dynamics in VU423 cells stably expressing mCherry-Rad52 reporter transfected with the indicated miRNA.

(D) Quantification of Idu/Cldu lengths in Kuramochi cells transfected with control-miR or miR-493-5p mimics with or without hydroxyurea treatment (left panel). Schematic of labeling cells with Cldu and Idu to study replication fork degradation (right panel) is shown.

For all panels, data are represented as mean ± SEM from three different experiments, n.s. represents p value > 0.05, *p value < 0.05, **p value < 0.01, ***p value < 0.001, and ****p value < 0.0001. See also Figure S4.

affects the other DSB repair pathways, C-NHEJ and alt-EJ, using the EJ5 and EJ2 reporter system, respectively (Figure 4A). *BRCA2* silencing did not have a significant impact on C-NHEJ or alt-EJ. We did not observe a change in alt-EJ in *BRCA2*-silenced cells overexpressing miR-493-5p. However, we did observe a modest but statistically significant increase in total NHEJ measured by the EJ5 reporter assay system in *BRCA2*-silenced cells overexpressing miR-493-5p, although there was no difference compared to non-*BRCA2*-silenced cells (Figure 4A). The decrease in HRR and SSA by expression of miR-493-5p is consistent with its impact on the DNA end resection machinery (*EXO1*, *MRE11*, and *BLM*). These results led us to hypothesize that miR-493-5p might potentiate PARPi and platinum resistance in *BRCA2* mutant cells, not by restoring HRR but by muting the otherwise hyperactive SSA pathway and promoting repair by NHEJ.

## miR-493-5p Stabilizes Replication Fork in *BRCA2* Mutant Cells

Stabilization of DNA replication fork has recently emerged as a mechanism of PARPi and platinum resistance in *BRCA2* mutant cells. *CHD4* (Guillemette et al., 2015), *MRE11* (Ding et al., 2016; Schlacher et al., 2011), and *EXO1* (Lemaçon et al., 2017) are factors that contribute to destabilizing the replication fork in *BRCA2* mutant cells and are recruited/stabilized at the fork by *PTIP* (Ray Chaudhuri et al., 2016). It is worth noting that silencing *PTIP* causes resistance to olaparib and cisplatin in Kuramochi and OVSAHO cells at a scale comparable to the impact of miR-493-5p (Figure S4C). Because top hits from our transcriptomic analysis include nucleases, in particular MRE11 and EXO1, we proceeded to quantify the effect of miR-493-5p on replication fork stability using DNA fiber analysis. To study replication fork dynamics after overexpression of miR-493-5p in

*BRCA2*-mutated Kuramochi cells, cells were labeled with Cldu for 1.5 hr and Idu for 2 hr followed by hydroxyurea (HU) exposure for 3 hr. In *BRCA2* mutant Kuramochi cells treated with control miRNA, HU significantly decreased the ratio of Idu/Cldu consistent with shortening of the Idu replication tract (Figure 4D). However, in Kuramochi cells overexpressing miR-493-5p, HU exposure did not cause any significant change in Idu/Cldu ratio, suggesting a potential role for miR-493-5p in regulating genes responsible for replication fork protection in *BRCA2*-mutated cells (Figure 4D). Results from our microarray profiling (Figure 3A) and DNA fiber analysis provide strong evidence that PARPi and platinum resistance induced by miR-493-5p in *BRCA2* mutant cells may be a result of DNA replication fork stabilization achieved through downregulation of *MRE11* and *CHD4*.

### miR-493-5p May Impact Multiple Genome-Stabilizing Pathways

As stated above, top hits from our bioinformatics analysis identified targets for miR-493-5p like *FEN1*, *SSRP1*, and *RNASEH2A* that are known to play a role in R-loop processing and ribonucleotide excision repair (RER) pathway (Figure 5A; Herrera-Moyano et al., 2014; Teasley et al., 2015; Williams et al., 2016) To investigate the impact of miR-493-5p on R-loop processing, we used a monoclonal S9.6 antibody that specifically detects RNA-DNA hybrids. We measured S9.6 signal intensity in miR-493-5p-overexpressing *BRCA2*-mutated VU423 cells and detected a significant increase in R-loops (Figure 5B), which was abolished upon transient overexpression of GFP-tagged RNaseH1.

To determine whether RER pathway members identified from our analysis play a role in mediating chemo-resistance in *BRCA2* mutant cells, we silenced *RNASEH2A*, *SSRP1*, or *FEN1* in *BRCA2* mutant cells. Loss of these genes induces PARPi and platinum resistance (Figure 5C). Finally, we analyzed the correlation of *RNASEH2A*, *FEN1*, and *SSRP1* expression with disease-free survival after platinum chemotherapy in *BRCA2* mutant carcinomas in TCGA. Consistent with the notion that miR-493-5p-mediated suppression of these factors promotes platinum resistance in *BRCA2* mutant carcinomas, we observe a striking inverse correlation of *RNASEH2A*, *FEN1*, and *SSRP1* with outcome after platinum chemotherapy only in *BRCA2* mutant carcinomas and not in *BRCA1* mutant carcinomas (Figures 5D and S5A). Together, these results suggest that miR-493-5p may mediate response to PARPi and platinum-based drugs in *BRCA2*-mutated tumors by regulating genes that play an important role in diverse repair pathways.

## DISCUSSION

We report miR-493-5p as a mediator of platinum and PARPi resistance in *BRCA2*-mutated ovarian carcinoma. mir-493-5p has been previously implicated in the process of carcinogenesis by regulating a number of target genes, including c-MET, EGFR (Wang et al., 2017), integrin subunit beta 1 (ITGB1) (Liang et al., 2017), and fucosyltransferase IV (FUT4) (Zhao et al., 2016) in various tumor types, including breast, prostate, and lung cancers. However, no previous implication of miR-493-5p in DNA repair or responsiveness to chemotherapy has been reported. We identified miR-493-5p by next-generation sequencing of small RNAs extracted from primary and recurrent *BRCA1/2*-mutated ovarian carcinomas, which was then validated in the TCGA ovarian cancer dataset (Cancer Genome Atlas Research Network, 2011). None of these tumors harbored secondary *BRCA1/2* mutations, suggesting that the association between miR-493-5p and platinum resistance could not have been confounded by presence of secondary *BRCA1/2* mutations. In addition to the findings from patient tumor samples, miR-493-5p conferred platinum and PARPi resistance in *BRCA2*-mutated, but not *BRCA1*-mutated, cell lines *in vitro* and was found to be significantly overexpressed in approximately one-third of *Brca2*-deficient KB2P mammary tumor models (13 of 40 resistant models) with acquired *in vivo* resistance to PARPi AZD2461 compared to paired naive untreated tumors. It is important to underscore that secondary *Brca2* mutations or Pgp overexpression cannot explain the acquired resistance of KB2P model to AZD2461 because the KB2P model harbors biallelic deletion in *Brca2* and PARPi AZD2461 is not a P-glycoprotein (Pgp) substrate.

Mechanistically, to identify clinically relevant gene targets of miR-493-5p, we performed gene expression profiling to identify genes that were significantly downregulated in *BRCA2*-mutated ovarian cancer cells transfected with miR-493-5p. The downregulated transcripts included many key genes required for genome stability, and several of these inversely correlated with expression of miR-493-5p in *BRCA2*-mutated ovarian carcinomas from TCGA dataset, thereby ensuring the clinical relevance of this interaction. Diminished transcript levels do not always lead to significant decrease in protein; therefore, we validated by immunoblot that indeed miR-493-5p downregulates the expression of these factors involved in DNA repair/replication and genomic stability. This approach identified several miR-493-5p targets that are involved in pathways that are relevant to the biology of *BRCA2*-mutated carcinomas as well as the development of platinum and PARPi resistance.

Stabilizing the replication fork is a recently identified mechanism of platinum and PARPi resistance in *BRCA2*-mutated carcinomas (Ray Chaudhuri et al., 2016). Beyond their role in DSB repair via HRR, *BRCA1* and *BRCA2* occupy an important role in limiting access of nucleases (such as *MRE11*) to single-strand DNA at stalled replication forks, thereby leading to replication fork protection. Recently, loss of *PTIP*, *CHD4*, and *EZH2* have been identified as a mechanism of resistance in *BRCA2*-deficient cells (Ding et al., 2016; Guillemette et al., 2015; Ray Chaudhuri et al., 2016; Rondinelli et al., 2017). Specifically, deficiency in *PTIP* and *CHD4* impedes recruitment of *MRE11*, thereby protecting stalled replication forks from nucleolytic degradation in *BRCA2* mutant cells. Two clinically relevant questions that emerge from these studies are (1) are these factors downregulated in *BRCA2* mutant carcinomas? (2) What is the mechanism by which the factors are suppressed? Here, we observed that miR-493-5p significantly downregulated *MRE11*, *CHD4*, and another nuclease *EXO1* in *BRCA2* mutant cells. Most importantly, consistent with these results, miR-493-5p preserved replication fork stability in *BRCA2*-mutated ovarian cancer cells.

We also show that miR-493-5p plays a role in regulating DSB repair pathway choice in *BRCA2* mutant cells. miR-493-5p decreased SSA and in consonant also significantly decreased

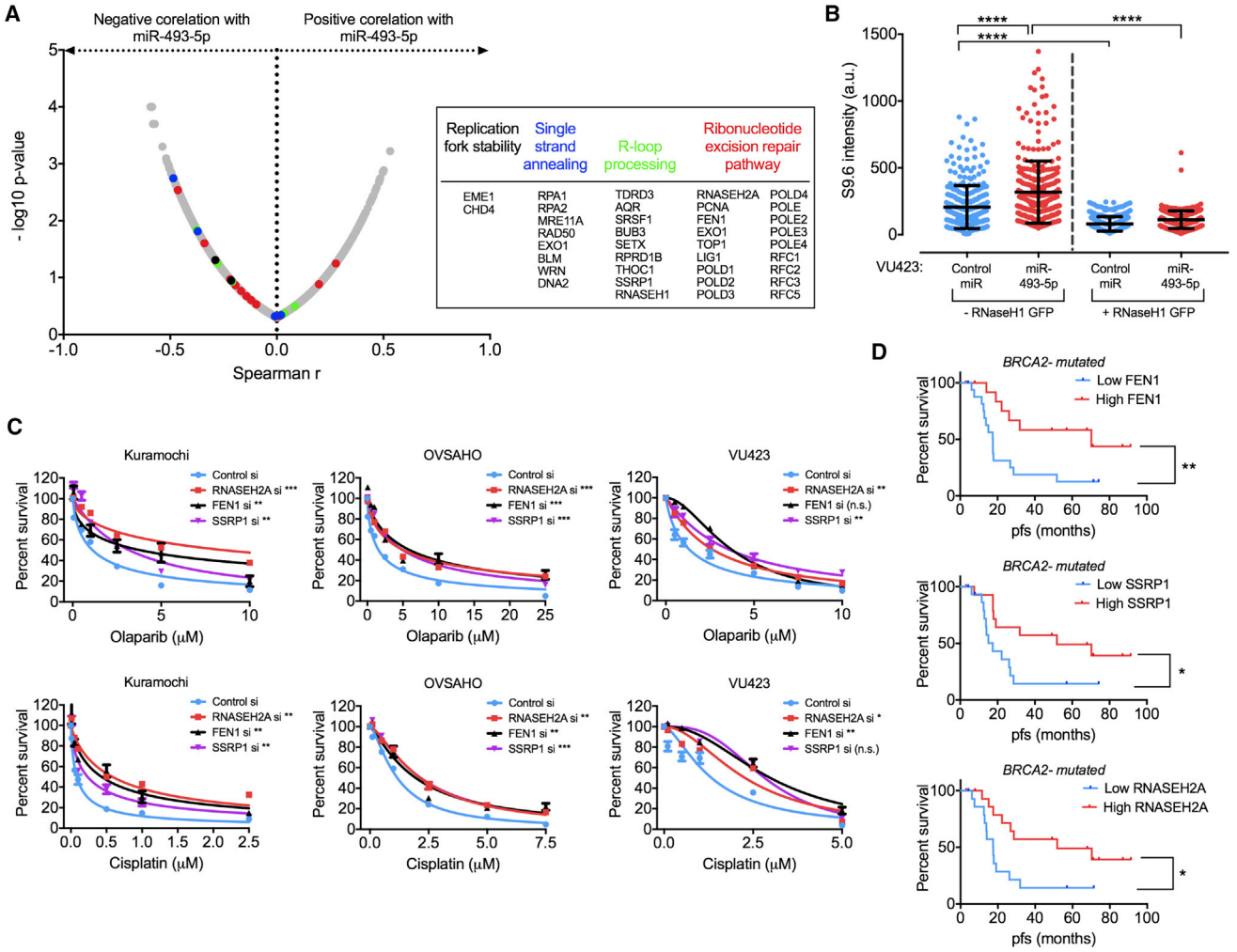


**Figure 5. miR-493-5p Has an Impact on Pathways Regulating R-Loop Processing and Ribonucleotide Excision Repair Pathway**

(A) Plot showing correlation of miR-493-5p with different pathways.

(B) Quantification of R-loops measured as S9.6 intensity in *BRCA2* mutant VU423 cells transfected with control-miR or miR-493-5p post-transfection with RNaseH1-GFP.

(C) Survival assays to assess the impact of *BRCA2* mutant Kuramochi, OVSAHO, and VU423 cells transfected with the indicated siRNA and treated with the indicated DNA-damaging agents.

(D) Progression-free survival for *BRCA2*-mutated HGSOC in the TCGA dataset segregated based on the median expression levels of *RNASEH2A*, *SSRP1*, and *FEN1*. Statistical significance was assessed by the log rank test.

For Figures 5B and 5C, data are represented as mean ± SEM from three different experiments, n.s. represents p value > 0.05, *p value < 0.05, **p value < 0.01, ***p value < 0.001, and ****p value < 0.0001. See also Figure S5.

levels of *BLM* and *EXO1* along with *MRE11*, which are key actors in DNA end resection, a critical step in SSA. Additionally, miR-493-5p did not rescue HRR, thereby eliminating restoration of HRR as a possible explanation of the observed platinum and PARPi resistance. These observations distinctly indicate that miR-493-5p impacts DNA repair pathway choice in *BRCA2* mutant cells and may mediate platinum and PARPi resistance by suppression of the highly mutagenic and genome-destabilizing SSA, which is otherwise hyperactive in *BRCA2* mutant cells.

Finally, our analysis identified *RNASEH2A*, *FEN1*, and *SSRP1* as miR-493-5p targets; these genes are known to be implicated in multiple genome-stabilizing pathways, including the degradation of transcriptionally generated R-loops (Herrera-Moyano et al., 2014; Teasley et al., 2015) and RER pathway. R-loops are an established source of genome instability and a potential driver of tumorigenesis (Aguilera and García-Muse, 2012; Aguilera and Gómez-González, 2017; Santos-Pereira and Aguilera, 2015; Sollier and Cimprich, 2015). The precise molecular mechanisms by which R-loops promote tumorigenesis remain unclear. A genome-wide examination of R-loop dynamics in different cell types from *BRCA1* mutation carriers revealed *BRCA1*-mutation-associated R-loops preferentially accumulate in luminal epithelial cells and at specific genomic loci leading to tumorigenesis (Zhang et al., 2017). Furthermore, in

*BRCA1*-deficient carcinomas, there is a significant enrichment of mutations at precise locations where *BRCA1* is predicted to suppress R-loops (Hatchi et al., 2015). *BRCA2* also plays a key role in removal of R-loops that are formed in transcriptionally active regions of the genome (Bhatia et al., 2014). So far, there is no information on whether R-loops impact response of *BRCA2*-deficient carcinomas to platinum drugs and PARPis. Based on our results, we speculate that an increase in R-loops might be a contributing factor to the chemo-resistance of *BRCA2*-deficient carcinomas.

Although both *BRCA1* and *BRCA2* are involved in HRR and loss of these factors confers PARPi sensitivity, expression of miR-493-5p induces platinum and PARPi resistance exclusively in *BRCA2*-mutated cells. It is noteworthy that the genomic landscape of *BRCA1* and *BRCA2* tumors is very different with very distinct chromosomal aberrations and mutational signatures (Nik-Zainal et al., 2016). Therefore, it is conceivable that, even if miR-493-5p targets the same pathways in *BRCA1* mutant carcinomas, it doesn't cause platinum and PARPi resistance due to other genetic/epigenetic differences with *BRCA2* mutant carcinomas. In conclusion, we report miR-493-5p as a mediator of platinum and PARPi resistance in *BRCA2*-mutated ovarian carcinomas. Our data suggest that miR-493-5p mediates chemotherapeutic response by targeting several genes in pathways that play an important role in the maintenance of genome stability. Our study highlights a previously unrecognized role for miR-493-5p as a potential biomarker of responsiveness to platinum and PARPis as well as a target for reversing platinum and PARPi resistance in *BRCA2*-mutated ovarian carcinomas.

## EXPERIMENTAL PROCEDURES

### miRNA Profiling and Survival Analysis

Exiqon miRNA profiling was used to identify miRNAs that are differentially expressed in 38 *BRCA1/2*-mutated carcinomas with known response to platinum therapy obtained from the University of Washington Gynecologic Oncology Tissue Bank, in which tissues are obtained from patients undergoing surgery for primary or recurrent ovarian carcinoma who provide informed consent according to an institutional review board (IRB)-approved protocol. These carcinomas were confirmed to not harbor *BRCA1/2* reversion mutations by sequencing. Normalized sequencing data counts for 953 miRNAs were available from Exiqon. Any miRNAs that were not detected in more than 19 of the carcinomas were not included in the final analysis. Expression values were standardized, following which miRNA levels were queried in refractory versus sensitive tumors. Independent samples t test with p value significance $<0.05$ was used as a statistical cutoff. 48 miRNAs were differentially expressed in refractory versus sensitive carcinomas (both directions). Overall survival data were queried for the available carcinomas, and log rank (Mantel-Cox) p value $<$ 0.05 was used as a statistical cutoff to identify miRNAs that have an effect on overall survival. We queried overall survival data for 38 carcinomas based on median cutoff of miRNA expression. 8 miRNAs significantly affect overall survival in 38 *BRCA1/2*-mutated tumors. Next, we queried the survival analysis for the 8 miRNAs identified to be differentially expressed and causing a significant effect on overall survival in *BRCA1/2*-mutated carcinomas in 2 subgroups: *BRCA1*-mutated carcinomas and *BRCA2*-mutated carcinomas. We utilized the TCGA cohort for validating our results observed in the University of Washington cohort. We queried the survival analysis for the 8 miRNA hits in 38 *BRCA1*-mutated carcinomas and 34 *BRCA2*-mutated carcinomas.

### Cell Survival Assays

For assessing cellular toxicity, cells were transfected with the indicated small interfering RNA (siRNA) or miRNA for 48 hr before plating cells into 96-well plates. The next day, DNA-damaging agents were added at the indicated concentrations. Cells were incubated with the drug containing media for 5 or 6 days before media was removed and replaced with drug-free media. Cells were incubated in drug-free media for 3 days before viability was measured using Cell-titer Glo reagent and assayed using a luminescence plate reader. Untreated and treated conditions were repeated in triplicates for each experiment, and each experiment was repeated at least three times. Viability for each drug concentration was normalized using untreated condition. Graphs represent percentage of surviving cells for each condition ± SEM.

### mir-493-5p Levels in KB2P Tumor Models

RNA extracted from 19 naive and 40 resistant KB2P p53−/− *Brca2*−/− mammary tumor models using Trizol reagent (Invitrogen) was reverse transcribed using Universal cDNA synthesis kit II (Exiqon). Resulting cDNA was used to query miR-493-5p levels using ExiLENT SYBR Green master mix and LNA qPCR primers designed to accurately detect mmu-miR-493-5p in an Applied Biosystems qPCR machine. All reagents were used according to manufacturer instructions. miR-493-5p expression level was normalized to expression of U6 small nuclear RNA (snRNA) using the ΔCt method. Graphs represent expression values of miR-493-5p for each resistant tumor relative to miR-493-5p levels for its naive tumor counterpart and are indicated as average ± SEM. Each reaction had at least 4 replicates. LNA qPCR primer target sequence is as described on Exiqon's website.

The U6snRNA target sequence (targets hsa, mmu U6snRNA) is as follows: GUGCUCGCUUCGGCAGCACAUAUACUAAAAUUGGAACGAUACAGAGAAGAUUAGCAUGGCCCCUGCGCAAGGAUGACACGCAAAUUCGUGAAGCGUUCCAUAUUUUU.

The miR-493-5p target sequence (targets mmu miR-493-5p) is as follows: UUGUACAUGGUAGGCUUUC.

### Microarray Profiling and Data Analysis

RNA was extracted from *BRCA2* mutant Kuramochi cells transfected twice with either control-miR or miR-493-5p and submitted for whole-transcriptome profiling to the Molecular Biology Core Facilities at Dana-Farber Cancer Institute. Affymetrix Human Transcriptome Array (HTA) 2.0 platform was used for quantification of transcripts. Pre-processing of Affymetrix CEL files was performed using Expression Console software application (Affymetrix) using the robust multi-chip analysis (RMA) algorithm, which performs background adjustment, quantile normalization, and probe-level summarization. A total of 67,528 transcripts were detected in the microarray, of which 44,699 were probed in coding regions of genome and 22,829 were probed in non-coding regions of genome. Fold change (linear and log 2) for each transcript detected was calculated for control versus miR-493-5p-transfected cells from raw values. For the purpose of our analysis, we focused on transcripts queried in the coding regions of the genome. (ANOVA p value $< 0.05$ and false discovery rate [FDR] p value $< 0.20$ [Benajmini-Hochberg method] were used for statistical significance). For every gene that passed the statistical significance tests, publicly available TCGA mRNA expression *Z* score data along with the microRNA expression *Z* scores for miR-493-5p were downloaded from http://cBioportal.org. Clinical characteristics for carcinomas in the TCGA dataset along with *BRCA1* and *BRCA2* mutational information was also downloaded from http://cBioportal.org. Thirty-four carcinomas harboring a *BRCA2* mutation were isolated from the cohort (two tumors: TCGA-13-1512-01 and TCGA-23-1026-01 have both a *BRCA1* and *BRCA2* mutation and are considered to be hyper-mutated and not included in the analysis). Non-parametric Spearman correlation coefficient and one-tailed p value (95% confidence interval) was calculated for each gene and miR-493-5p pair for the 34 *BRCA2*-mutated samples. Quadrant-based scatterplot was created by plotting log2 fold change (x axis; control versus miR493 transfected) against Spearman r correlation coefficient values for genes with a significant correlation to miR-493-5p in the TCGA dataset. Each quadrant (labeled in Figure 3B) was classified based on the direction and magnitude of change or correlation for each gene. All necessary calculations were performed using Microsoft Excel, SPSS Statistics v24, and Graph Pad Prism v7.0.c.

### Reporter Assays

HRR, SSA, alt-EJ, and total NHEJ were measured using U2OS-based reporter assay systems as described previously. Briefly, cells were seeded in 6-well

plates and reverse transfected with the indicated siRNA, miRNA, or combination of both. 24 hr after transfection, cells were incubated with Isce1 adenovirus for 1 hr in FBS-free media, following which cells are incubated for 48 hr in FBS-containing media before harvesting for flow cytometry analysis. Activity of each reporter system was determined by fluorescence-activated cell sorting (FACS) quantification of GFP-positive cells. Each graph represents relative mean values ± SEM for each condition calculated by normalizing each condition to control transfected cells. Each experiment was repeated at least three times.

### Cell Line Construction

pEF1α-mcherry-Rad52 plasmid was kindly provided by Dr. Galit Lahav. Stable cell line expressing the plasmid was generated by transfecting VU423 cells using Fugene 6 followed by selection in hygromycin-containing media.

### Immunofluorescence

For Rad51 foci experiments, cells were transfected with indicated siRNA or miRNA or combination of both 48 hr before irradiation 5 Gy (gamma-IR). Cells were fixed 6 hr post-irradiation with 1% paraformaldehyde and 0.5% Triton X-100 for 30 min. Bovine serum albmin-Triton X-100-goat serum (BTG) buffer containing 1 mg/mL BSA, 0.1% Triton X-100, 3% goat serum, and 1 mM EDTA in PBS was used for blocking and to dilute primary (1°) and secondary (2°) antibodies. Coverslips containing cells were blocked in BTG buffer for 1 hr (room temperature), followed by overnight incubation in 1° antibody (4°C), three PBS washes, 1-hr incubation with 2° antibody (room temperature), and three washes. Coverslips were mounted with DAPI-containing mounting media (Southern Biotech). Number of foci per cell was quantified using publicly available cell image analysis software Cell Profiler (Broad Institute). More than 200 cells were imaged and quantified for number of foci for each condition. Graphs represent the raw values for number of foci for each condition. Error bars represented are SEM for each condition.

### DNA Fiber Assay

DNA fiber analysis was performed as described before (Nieminuszczy et al., 2016). Briefly, *BRCA2* mutant Kuramochi cells were transfected with either control-miR or miR-493-5p for 48 hr followed by incubation with chlorodeoxyuridine (Cldu) for 1.5 hr followed by incubation with iododeoxyuridine (Idu) for 2 hr followed by treatment with either DMSO or 4 mM hydroxyurea for 3 hr. Cells were spotted on a slide followed by lysis with lysis buffer (200 mM Tris-HCl [pH 5.5], 50 mM EDTA, and 0.5% SDS), followed by 120-min incubation with 2.5 M hydrochloric acid. After three washes in water, slides are processed for immunofluorescence. Slides were incubated with blocking buffer (1% BSA in PBS) for 1 hr at room temperature followed by incubation with primary antibody for 1 hr at 37°C. Slides were washed three times in PBS followed by incubation with secondary antibody for 1 hr at 37°C. Coverslips were mounted on slides with DAPI-containing mounting media (Southern Biotech). At least 100 fibers were counted per condition. Images were analyzed using ImageJ software. Ratio of Idu fiber length/Cldu fiber length was used as a measure of fiber degradation. Primary antibodies used for this experiment were as follows: rat anti-bromodeoxyuridine (BrdU) specific to Cldu (Abcam; ab6326; 1:125) and mouse anti-BrdU specific to Idu (BD Biosciences; 347580; 1:50). Secondary antibodies used for this experiment were as follows: goat anti-rat immunoglobulin G (IgG) Alexa 488 (Life Technologies; A-11006; 1:250) and donkey anti-mouse IgG Alexa Fluor 594 (Life Technologies; A-21203; 1:250).

## SUPPLEMENTAL INFORMATION

Supplemental Information includes five figures and one table and can be found with this article online at https://doi.org/10.1016/j.celrep.2018.03.038.

## ACKNOWLEDGMENTS

D.C. is supported by R01CA208244 (NCI) and R01CA142698-07 (NCI), a Leukemia and Lymphoma Society Scholar Grant, the Claudia Adams Barr Program for Innovative Cancer Research, the Robert and Deborah First Family Fund Award, and Tina's Wish Foundation. D.C. and P.K. are supported by DOD W81XWH-15-0564/OC140632.

## AUTHOR CONTRIBUTIONS

K.M. conducted most of the experiments with assistance from W.F. K.M., A.D., and P.D. conducted microscopy experiments and intensity quantifications. K.M., P.A.K., and D.C. conducted all of the statistical analyses. E.G. conducted the experiments with the *Brca2* mouse model under the supervision of S.R. and J.J. The clinical samples were provided by E.M.S., and U.M. helped with analysis and interpretation of clinical data. K.M., D.C., and P.A.K. wrote the manuscript. D.C. and P.A.K. conceived the study.

## DECLARATION OF INTERESTS

The authors declare no competing interests.

Received: October 12, 2017
Revised: February 5, 2018
Accepted: March 10, 2018
Published: April 3, 2018

## REFERENCES

Aguilera, A., and García-Muse, T. (2012). R loops: from transcription byproducts to threats to genome stability. Mol. Cell *46*, 115–124.

Aguilera, A., and Gómez-González, B. (2017). DNA-RNA hybrids: the risks of DNA breakage during transcription. Nat. Struct. Mol. Biol. *24*, 439–443.

Aly, A., and Ganesan, S. (2011). BRCA1, PARP, and 53BP1: conditional synthetic lethality and synthetic viability. J. Mol. Cell Biol. *3*, 66–74.

Bennardo, N., Cheng, A., Huang, N., and Stark, J.M. (2008). Alternative-NHEJ is a mechanistically distinct pathway of mammalian chromosome break repair. PLoS Genet. *4*, e1000110.

Bhatia, V., Barroso, S.I., García-Rubio, M.L., Tumini, E., Herrera-Moyano, E., and Aguilera, A. (2014). BRCA2 prevents R-loop accumulation and associates with TREX-2 mRNA export factor PCID2. Nature *511*, 362–365.

Bouwman, P., Aly, A., Escandell, J.M., Pieterse, M., Bartkova, J., van der Gulden, H., Hiddingh, S., Thanasoula, M., Kulkarni, A., Yang, Q., et al. (2010). 53BP1 loss rescues BRCA1 deficiency and is associated with triple-negative and BRCA-mutated breast cancers. Nat. Struct. Mol. Biol. *17*, 688–695.

Bunting, S.F., Callén, E., Wong, N., Chen, H.T., Polato, F., Gunn, A., Bothmer, A., Feldhahn, N., Fernandez-Capetillo, O., Cao, L., et al. (2010). 53BP1 inhibits homologous recombination in Brca1-deficient cells by blocking resection of DNA breaks. Cell *141*, 243–254.

Cancer Genome Atlas Research Network (2011). Integrated genomic analyses of ovarian carcinoma. Nature *474*, 609–615.

Choi, Y.E., Pan, Y., Park, E., Konstantinopoulos, P., De, S., D'Andrea, A., and Chowdhury, D. (2014). MicroRNAs down-regulate homologous recombination in the G1 phase of cycling cells to maintain genomic stability. eLife *3*, e02445.

Choi, Y.E., Meghani, K., Brault, M.E., Leclerc, L., He, Y.J., Day, T.A., Elias, K.M., Drapkin, R., Weinstock, D.M., Dao, F., et al. (2016). Platinum and PARP inhibitor resistance due to overexpression of microRNA-622 in BRCA1-mutant ovarian cancer. Cell Rep. *14*, 429–439.

Ding, X., Ray Chaudhuri, A., Callen, E., Pang, Y., Biswas, K., Klarmann, K.D., Martin, B.K., Burkett, S., Cleveland, L., Stauffer, S., et al. (2016). Synthetic viability by BRCA2 and PARP1/ARTD1 deficiencies. Nat. Commun. *7*, 12425.

Evers, B., Helleday, T., and Jonkers, J. (2010). Targeting homologous recombination repair defects in cancer. Trends Pharmacol. Sci. *31*, 372–380.

Feng, W., and Jasin, M. (2017). BRCA2 suppresses replication stress-induced mitotic and G1 abnormalities through homologous recombination. Nat. Commun. *8*, 525.

Guillemette, S., Serra, R.W., Peng, M., Hayes, J.A., Konstantinopoulos, P.A., Green, M.R., and Cantor, S.B. (2015). Resistance to therapy in BRCA2 mutant

cells due to loss of the nucleosome remodeling factor CHD4. Genes Dev. *29*, 489–494.

Hatchi, E., Skourti-Stathaki, K., Ventz, S., Pinello, L., Yen, A., Kamieniarz-Gdula, K., Dimitrov, S., Pathania, S., McKinney, K.M., Eaton, M.L., et al. (2015). BRCA1 recruitment to transcriptional pause sites is required for R-loop-driven DNA damage repair. Mol. Cell *57*, 636–647.

Herrera-Moyano, E., Mergui, X., García-Rubio, M.L., Barroso, S., and Aguilera, A. (2014). The yeast and human FACT chromatin-reorganizing complexes solve R-loop-mediated transcription-replication conflicts. Genes Dev. *28*, 735–748.

Jaspers, J.E., Sol, W., Kersbergen, A., Schlicker, A., Guyader, C., Xu, G., Wessels, L., Borst, P., Jonkers, J., and Rottenberg, S. (2015). BRCA2-deficient sarcomatoid mammary tumors exhibit multidrug resistance. Cancer Res. *75*, 732–741.

Jonkers, J., Meuwissen, R., van der Gulden, H., Peterse, H., van der Valk, M., and Berns, A. (2001). Synergistic tumor suppressor activity of BRCA2 and p53 in a conditional mouse model for breast cancer. Nat. Genet. *29*, 418–425.

Konstantinopoulos, P.A., Ceccaldi, R., Shapiro, G.I., and D'Andrea, A.D. (2015). Homologous recombination deficiency: exploiting the fundamental vulnerability of ovarian cancer. Cancer Discov. *5*, 1137–1154.

Lai, X., Broderick, R., Bergoglio, V., Zimmer, J., Badie, S., Niedzwiedz, W., Hoffmann, J.S., and Tarsounas, M. (2017). MUS81 nuclease activity is essential for replication stress tolerance and chromosome segregation in BRCA2-deficient cells. Nat. Commun. *8*, 15983.

Lemaçon, D., Jackson, J., Quinet, A., Brickner, J.R., Li, S., Yazinski, S., You, Z., Ira, G., Zou, L., Mosammaparast, N., and Vindigni, A. (2017). MRE11 and EXO1 nucleases degrade reversed forks and elicit MUS81-dependent fork rescue in BRCA2-deficient cells. Nat. Commun. *8*, 860.

Liang, Z., Kong, R., He, Z., Lin, L.Y., Qin, S.S., Chen, C.Y., Xie, Z.Q., Yu, F., Sun, G.Q., Li, C.G., et al. (2017). High expression of miR-493-5p positively correlates with clinical prognosis of non small cell lung cancer by targeting oncogene ITGB1. Oncotarget *8*, 47389–47399.

Lord, C.J., and Ashworth, A. (2016). BRCAness revisited. Nat. Rev. Cancer *16*, 110–120.

Matulonis, U.A., Penson, R.T., Domchek, S.M., Kaufman, B., Shapira-Frommer, R., Audeh, M.W., Kaye, S., Molife, L.R., Gelmon, K.A., Robertson, J.D., et al. (2016). Olaparib monotherapy in patients with advanced relapsed ovarian cancer and a germline BRCA1/2 mutation: a multistudy analysis of response rates and safety. Ann. Oncol. *27*, 1013–1019.

Mirza, M.R., Monk, B.J., Herrstedt, J., Oza, A.M., Mahner, S., Redondo, A., Fabbro, M., Ledermann, J.A., Lorusso, D., Vergote, I., et al.; ENGOT-OV16/NOVA Investigators (2016). Niraparib maintenance therapy in platinum-sensitive, recurrent ovarian cancer. N. Engl. J. Med. *375*, 2154–2164.

Moskwa, P., Buffa, F.M., Pan, Y., Panchakshari, R., Gottipati, P., Muschel, R.J., Beech, J., Kulshrestha, R., Abdelmohsen, K., Weinstock, D.M., et al. (2011). miR-182-mediated downregulation of BRCA1 impacts DNA repair and sensitivity to PARP inhibitors. Mol. Cell *41*, 210–220.

Nieminuszczy, J., Schwab, R.A., and Niedzwiedz, W. (2016). The DNA fibre technique - tracking helicases at work. Methods *108*, 92–98.

Nik-Zainal, S., Davies, H., Staaf, J., Ramakrishna, M., Glodzik, D., Zou, X., Martincorena, I., Alexandrov, L.B., Martin, S., Wedge, D.C., et al. (2016). Landscape of somatic mutations in 560 breast cancer whole-genome sequences. Nature *534*, 47–54.

Norquist, B., Wurz, K.A., Pennil, C.C., Garcia, R., Gross, J., Sakai, W., Karlan, B.Y., Taniguchi, T., and Swisher, E.M. (2011). Secondary somatic mutations restoring BRCA1/2 predict chemotherapy resistance in hereditary ovarian carcinomas. J. Clin. Oncol. *29*, 3008–3015.

Oplustil O'Connor, L., Rulten, S.L., Cranston, A.N., Odedra, R., Brown, H., Jaspers, J.E., Jones, L., Knights, C., Evers, B., Ting, A., et al. (2016). The PARP inhibitor AZD2461 provides insights into the role of PARP3 inhibition for both synthetic lethality and tolerability with chemotherapy in preclinical models. Cancer Res. *76*, 6084–6094.

Patch, A.M., Christie, E.L., Etemadmoghadam, D., Garsed, D.W., George, J., Fereday, S., Nones, K., Cowin, P., Alsop, K., Bailey, P.J., et al.; Australian Ovarian Cancer Study Group (2015). Whole-genome characterization of chemoresistant ovarian cancer. Nature *521*, 489–494.

Ray Chaudhuri, A., Callen, E., Ding, X., Gogola, E., Duarte, A.A., Lee, J.E., Wong, N., Lafarga, V., Calvo, J.A., Panzarino, N.J., et al. (2016). Replication fork stability confers chemoresistance in BRCA-deficient cells. Nature *535*, 382–387.

Rondinelli, B., Gogola, E., Yücel, H., Duarte, A.A., van de Ven, M., van der Sluijs, R., Konstantinopoulos, P.A., Jonkers, J., Ceccaldi, R., Rottenberg, S., and D'Andrea, A.D. (2017). EZH2 promotes degradation of stalled replication forks by recruiting MUS81 through histone H3 trimethylation. Nat. Cell Biol. *19*, 1371–1378.

Sakai, W., Swisher, E.M., Karlan, B.Y., Agarwal, M.K., Higgins, J., Friedman, C., Villegas, E., Jacquemont, C., Farrugia, D.J., Couch, F.J., et al. (2008). Secondary mutations as a mechanism of cisplatin resistance in BRCA2-mutated cancers. Nature *451*, 1116–1120.

Sakai, W., Swisher, E.M., Jacquemont, C., Chandramohan, K.V., Couch, F.J., Langdon, S.P., Wurz, K., Higgins, J., Villegas, E., and Taniguchi, T. (2009). Functional restoration of BRCA2 protein by secondary BRCA2 mutations in BRCA2-mutated ovarian carcinoma. Cancer Res. *69*, 6381–6386.

Santos-Pereira, J.M., and Aguilera, A. (2015). R loops: new modulators of genome dynamics and function. Nat. Rev. Genet. *16*, 583–597.

Schlacher, K., Christ, N., Siaud, N., Egashira, A., Wu, H., and Jasin, M. (2011). Double-strand break repair-independent role for BRCA2 in blocking stalled replication fork degradation by MRE11. Cell *145*, 529–542.

Sollier, J., and Cimprich, K.A. (2015). Breaking bad: R-loops and genome integrity. Trends Cell Biol. *25*, 514–522.

Stark, J.M., Pierce, A.J., Oh, J., Pastink, A., and Jasin, M. (2004). Genetic steps of mammalian homologous repair with distinct mutagenic consequences. Mol. Cell. Biol. *24*, 9305–9316.

Swisher, E.M., Sakai, W., Karlan, B.Y., Wurz, K., Urban, N., and Taniguchi, T. (2008). Secondary BRCA1 mutations in BRCA1-mutated ovarian carcinomas with platinum resistance. Cancer Res. *68*, 2581–2586.

Swisher, E.M., Lin, K.K., Oza, A.M., Scott, C.L., Giordano, H., Sun, J., Konecny, G.E., Coleman, R.L., Tinker, A.V., O'Malley, D.M., et al. (2017). Rucaparib in relapsed, platinum-sensitive high-grade ovarian carcinoma (ARIEL2 Part 1): an international, multicentre, open-label, phase 2 trial. Lancet Oncol. *18*, 75–87.

Teasley, D.C., Parajuli, S., Nguyen, M., Moore, H.R., Alspach, E., Lock, Y.J., Honaker, Y., Saharia, A., Piwnica-Worms, H., and Stewart, S.A. (2015). Flap endonuclease 1 limits telomere fragility on the leading strand. J. Biol. Chem. *290*, 15133–15145.

Wang, S., Wang, X., Li, J., Meng, S., Liang, Z., Xu, X., Zhu, Y., Li, S., Wu, J., Xu, M., et al. (2017). c-Met, CREB1 and EGFR are involved in miR-493-5p inhibition of EMT via AKT/GSK-3β/Snail signaling in prostate cancer. Oncotarget *8*, 82303–82313.

Williams, J.S., Lujan, S.A., and Kunkel, T.A. (2016). Processing ribonucleotides incorporated during eukaryotic DNA replication. Nat. Rev. Mol. Cell Biol. *17*, 350–363.

Xu, G., Chapman, J.R., Brandsma, I., Yuan, J., Mistrik, M., Bouwman, P., Bartkova, J., Gogola, E., Warmerdam, D., Barazas, M., et al. (2015). REV7 counteracts DNA double-strand break resection and affects PARP inhibition. Nature *521*, 541–544.

Zhang, X., Chiang, H.C., Wang, Y., Zhang, C., Smith, S., Zhao, X., Nair, S.J., Michalek, J., Jatoi, I., Lautner, M., et al. (2017). Attenuation of RNA polymerase II pausing mitigates BRCA1-associated R-loop accumulation and tumorigenesis. Nat. Commun. *8*, 15908.

Zhao, L., Feng, X., Song, X., Zhou, H., Zhao, Y., Cheng, L., and Jia, L. (2016). miR-493-5p attenuates the invasiveness and tumorigenicity in human breast cancer by targeting FUT4. Oncol. Rep. *36*, 1007–1015.